

# Unusual Regioselective Electrophilic Substitutions in Quinoline Foldamers: Conceptual DFT and Frontier Molecular Orbital Analysis Reveal the Crucial Role of Folding and Substituents

Madishetti Shravani,<sup>[a]</sup> Shanigaram Balaiah,<sup>[b]</sup> Kolupula Srinivas,<sup>\*,[a]</sup> K. Bhanuprakash,<sup>[b]</sup> and Ivan Huc<sup>[c, d]</sup>

We carried out a detailed computational investigation of an earlier experimentally observed, unusual, regioselective, electrophilic halogenation in helically folded quinoline oligoamides. In the experimental studies, halogenation occurred selectively at a given monomer of a foldamer substituted with electron-withdrawing groups at the N terminus, although apparently identical reactive sites were available to react with the incoming electrophile. On the other hand, the selectivity was lost with weakly electron-donating groups. To gain an insight into the regioselective preference of bromination in quinoline foldamers, conceptual DFT was used to calculate the local nucleophilicity index of various foldamers of different sizes and with different substituents, and it was found that the predicted reaction centers were in line with the experimental results. Frontier molecular orbital analysis was used to understand this

behavior. A detailed study of the hypothetical linear conformation of the tetramer for comparison with the folded conformation was carried out. In the case of a linear conformer, the HOMO is localized on specific monomers irrespective of substitution, but upon folding delocalization is observed, which is larger for the weakly electron-donating groups when compared with the electron-withdrawing groups. In the case of strongly donating groups there is no delocalization, even upon folding. The behavior remains the same when the size of the helix is increased (octamer). Thus, it is clearly seen in this work that the combined effects of conformations and substituents dictate the regioselectivity in the folded oligoamides; this knowledge will have a profound effect on the field of foldamer chemistry.

## 1. Introduction

The structural intricacy and unmatched functions of molecules found in nature has inspired many researchers around the globe. To unravel the mystery behind the meticulous execution of the duties of biomacromolecules, scientists may investigate natural systems directly or use mimetic models.<sup>[1–6]</sup> Foldamers are one such mimetic model. The well-defined architectures (often helically folded), relative ease of synthesis, and controlled dynamics of foldamers have attracted the attention of many research groups.<sup>[7–10]</sup> This emerging and exciting area has witnessed remarkable growth in terms of tuning the shape and diameter of helical structures, chirality induction, encapsulation of small molecules, and the development of therapeutically significant entities.<sup>[11,12]</sup> To design a functional foldamer, a compact molecular structure is an important prerequisite. Although research concerning structural aspects of small foldamers is advanced, the design of artificial protein-like objects with tailored functions, such as drug-delivery agents or enzyme-like catalysts, is a long-standing goal.<sup>[7–15]</sup> Because foldamers are potential mimetics of protein structure, enzyme-like functions, namely, remarkable substrate selectivity, rate enhancements, and regioselectivity through supramolecular interactions, are anticipated in the coming years.<sup>[16–20]</sup> To prompt enzyme-like behavior, two strategies may be envisaged: 1) to craft an enzyme-like environment in a host designed to bind the sub-

strate; and 2) to create a distinctive environment on the substrate itself such that it triggers an intramolecular reaction without applying any host.<sup>[12,16–21]</sup> A great deal of research has been focused on the former approach; nevertheless, the latter strategy is simpler and seems to be promising because it does not require any host or protecting groups for selectivity and

[a] M. Shravani, Dr. K. Srinivas  
National Institute of Pharmaceutical Education  
and Research (NIPER), Hyderabad,  
Balanagar, Hyderabad 500037 (India)  
Fax: (+91) 40-2307 3751  
E-mail: skolupula@niperhyd.ac.in

[b] S. Balaiah, Dr. K. Bhanuprakash  
Inorganic and Physical Chemistry Division  
Indian Institute of Chemical Technology  
Tarnaka, Hyderabad 500607 (India)

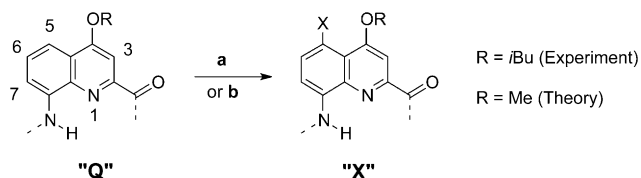
[c] Dr. I. Huc  
Université de Bordeaux, CBMN UMR 5248  
Institut Européen de Chimie et Biologie  
2 rue Robert Escarpit, 33607 Pessac Cedex (France)

[d] Dr. I. Huc  
CNRS, CBMN UMR 5248  
Institut Européen de Chimie et Biologie  
2 rue Robert Escarpit, 33607 Pessac Cedex (France)

 Supporting information for this article is available on the WWW under <http://dx.doi.org/10.1002/cphc.201200397>.

specificity.<sup>[22,23]</sup> Indeed, avoiding using a host and/or protecting groups is one of the greener approaches in organic synthesis and important contributions in this area have been published recently.<sup>[24]</sup> For example, Guthrie and Tovar have reported regioselective reactions on a crowded aromatic system with mutually reactive sites, in which the conformation itself acts as a protecting group.<sup>[25]</sup> They further meticulously highlighted how the conformation impacted on  $\pi$  conjugation, and thus, the electronic properties, and its significance for the construction of complex molecules without the aid of protecting groups.<sup>[26]</sup> It is an elegant strategy in which a molecule may itself attain a conformation, either by imposing steric factors or by folding, that offers desired reaction selectivity instead of making use of protecting groups and catalysis to elicit selectivity.<sup>[16–22,27]</sup>

In a recent report, we described the serendipitous discovery of unusually regioselective and enhanced electrophilic substitution reactions (ESRs) in helically folded oligoamides (Schemes 1 and 2) of 8-amino-2-quinolinecarboxylic acid (Q).<sup>[28]</sup> The folded oligomer possesses seemingly identical reaction



**Scheme 1.** Halogenation of quinoline oligoamides.<sup>[28]</sup> Reagents and conditions: a)  $\text{SOCl}_2$ , reflux, 30 min ( $\text{X} = \text{Cl}$ ); b) *N*-bromosuccinimide,  $\text{CDCl}_3$ , 40 °C ( $\text{X} = \text{Br}$ ). Abbreviated names,  $\text{O}_2\text{N}$ –,  $\text{NC}$ –, and so forth (in text) replace the terminal NH group.

sites on each monomer. Yet, selective bromination or chlorination occurs at a particular site on the folded structure under optimal conditions.<sup>[28]</sup> Specifically, oligomers with three or more quinoline units and a terminal  $-\text{NO}_2$  substituent in position 8 of the first quinoline unit undergo selective bromination on the third ring (Q3) from the N terminus. For example,  $\text{O}_2\text{N}$ – $\text{Q}_4$ – $\text{OMe}$  may be converted quantitatively on a multigram scale into  $\text{O}_2\text{N}$ – $\text{Q}_3\text{X}$ – $\text{OMe}$  (Figure 1 a). Even with a change in electron-withdrawing groups, for example,  $-\text{NO}_2$  substituted for a  $-\text{CN}$  group, the selectivity is retained (Figure 1 b). On the contrary, for  $\text{Ac}$ – $\text{Q}_4$ – $\text{OMe}$  one sees a mixture of brominated products (Figure 1 c). In addition, reaction rates were considerably faster in the longer, helically folded sequences than those in a simple flat di- or trimer, despite steric hindrance, which is greater in longer oligomers, as expected (Figure 1 d).<sup>[28]</sup>

Very few reports in the literature have dealt with rate acceleration or selective transformations within folded oligomers.<sup>[16–18,21–23,28–32]</sup> Moore and Heemstra reported the enhanced N-methylation of a pyridine nitrogen atom in *m*-phenyleneethylenes.<sup>[29]</sup> Huc and co-workers described the regioselective, enhanced N-oxidation of the terminal pyridine rings of helical pyridinecarboxamide oligomers.<sup>[30]</sup> Chen and co-workers reported the folding-induced selective hydrogenation of 9,10-

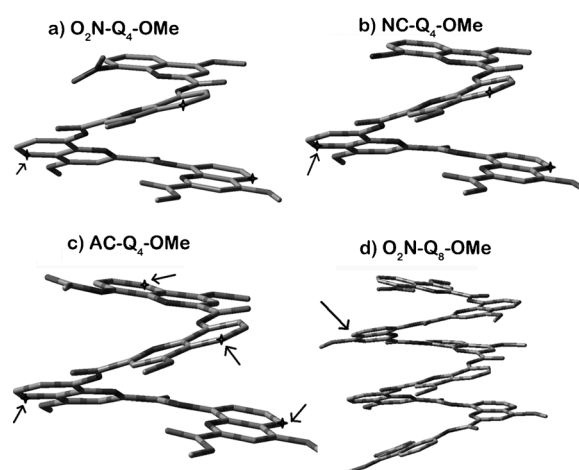
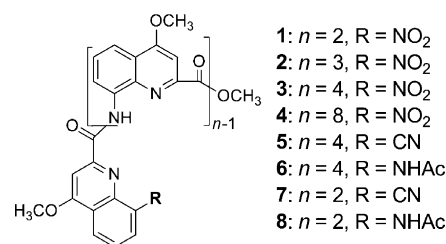


**Figure 1.** Folded quinoline oligoamides with different substituents. Arrows indicate sites of halogenation.<sup>[28]</sup>

anthraquinone within a helical oligomer.<sup>[31]</sup> Regioselectivity, in the above cases,<sup>[29–31]</sup> is a consequence of exposing a specific site to reagents and steric hindrance about other sites in the folded structure. However, in the case of the enhanced electrophilic substitution of quinoline oligoamides, regioselectivity occurs despite all potential reactive sites being comparably exposed to reagents.<sup>[28]</sup> An understanding of this unusual regioselective behavior (here direct mesomeric effects can be ruled out) is of interest because this would enhance our knowledge of reactivity in foldamers, which is of utmost importance. Thus, in this study, we make use of computational methods such as conceptual DFT and frontier molecular orbitals (FMOs) to explain this behavior.

Conceptual DFT has emerged as a strong tool to not only understand but also to predict regioselective reactions.<sup>[33–39]</sup> It has been applied with success in many earlier studies.<sup>[33–47]</sup> Hence, this was also our method of choice for this work. We carried out a detailed computational investigation into foldamers with various substitutions and sizes (Scheme 2). We then applied conceptual DFT to obtain the local nucleophilic index (LNI). The obtained LNI is in line with the experimental results, indicating that it can also be used to predict reactions in these molecules. FMO analysis clearly shows that localization and delocalization of the orbitals are influenced by folding and substituents.



**Scheme 2.** List of quinoline oligoamides for which the LNI is calculated in this study.

## Computational Methods

All of the calculations were carried out by using DFT methods implemented in the Gaussian 09 software.<sup>[46]</sup> All of the energy-minimized geometries in this study were obtained by using the hybrid density functional B3LYP at the default integration grid and MO6-2X/6-31G(d, p) basis set, as implemented in Gaussian 09. The theoretical singlet equilibrium structures were obtained when the maximum internal forces acting on all of the atoms and stresses were less than  $4.5 \times 10^{-4} \text{ eV \AA}^{-1}$  and  $1.01 \times 10^{-3} \text{ kbar}$ , respectively. The minima for the molecules up to the tetramer were confirmed by vibrational analysis.

The LNI values ( $N_k^-$ ) based on conceptual DFT indicated the intramolecular reactivity sequence or site selectivity in an individual chemical system, that is, they were relatively good descriptors for predicting regioselectivity within the molecule.<sup>[33–47]</sup> The LNI could be obtained from Fukui function indices and global nucleophilicity indices by using the relationship given in Equation (1):

$$N_k^- = N^* f_k^- \quad (1)$$

in which  $N$  is the global nucleophilicity index and  $f_k^-$  is the Fukui function for electrophilic attack on a specific site. LNI is an absolute scale that exclusively relies on the electronic characteristics of the nucleophile, and hence, is not dependent on the electrophilic partner. The Fukui function can be condensed to atoms by using electronic population analyses. Atomic populations were obtained by the natural population analysis (NPA) method implemented in Gaussian 09 software. The three-dimensional Fukui function is usually approximated by using a finite difference methodology. For LNI, the Fukui function given in Equation (2) was utilized:

$$f_k^- = \rho_N(k) - \rho_{N-1}(k) \quad (2)$$

in which  $\rho_N(k)$  is the NPA charge at atom  $k$  of a neutral molecule and  $\rho_{N-1}(k)$  is the NPA charge at atom  $k$  of the cation molecule.

The global nucleophilic reactivity descriptor ( $N$ ) can be calculated from Equation (3):<sup>[45]</sup>

$$N = \frac{1}{\omega^-} \quad (3)$$

$$\omega^- = \frac{(3I + A)^2}{16(I - A)}$$

in which  $I = E_{\text{HOMO}}$  = ionization potential (IP) and  $A = E_{\text{LUMO}}$  = electron affinity (EA). The reactivity indexes were computed from the B3LYP/6-311G(d, p) and MO62X/6-31G(d, p) basis sets and HOMO and LUMO energies were computed at the ground state of the molecules. Although there are other methods to quantify LNI, this method seems to be better able to distinguish between regioselective sites.<sup>[42]</sup>

Energies and selected MOs were generated by using Gaussian 09 software.

## 2. Results and Discussions

### 2.1. Structure and Geometry Optimization

Foldamers of quinoline oligoamides are known to take up two types of helical structures, P and M helices, in solution and the

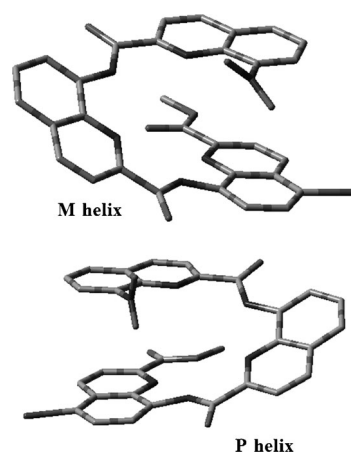


**Figure 2.** Crystal structures of M and P helices (enantiomers) of  $\text{O}_2\text{N-QQX-OMe}$  (isobutoxy side chains and hydrogen atoms are omitted for clarity).

solid state (Figure 2) for a trimer as an example.<sup>[15]</sup> Because P and M helices are enantiomers, to maintain clarity, and also for computational convenience, we carried out the studies reported herein only for P-helix foldamers (see Table S1 in the Supporting Information for more details). All of the molecules investigated in this study, for which experimental data (ESR)<sup>[28]</sup> are available, are shown in Scheme 2. For optimization, starting geometries of the nitro di-, tri-, and tetramers were taken from the crystal data<sup>[28]</sup> from which bromine atoms were removed and replaced with hydrogen atoms. For molecules with  $-\text{CN}$  ( $\text{NC-Q}_4\text{-OMe}$ ) and  $-\text{NHAc}$  ( $\text{Ac-Q}_4\text{-OMe}$ ) groups, we replaced the terminal  $-\text{NO}_2$  by these groups and reoptimized the structures. Isobutoxy side chains in the crystal structures were modified to methoxy groups for simplification of the structure and in view of the computational cost. Energy minimization was carried out at the B3LYP/6-311G(d, p) and MO6-2X/6-31G(d, p) levels for all oligoamides, except for the nitro octamer ( $\text{O}_2\text{N-Q}_8\text{-OMe}$ ). The structure of the latter was extracted from the crystal structure of the monobrominated nitro octamer ( $\text{O}_2\text{N-QQXQ}_5\text{-OMe}$ ) by replacing the bromine atom with hydrogen and performing the optimization at the B3LYP/3-21G level only (for these larger oligoamides, convergence was achieved with the MO6-2X/3-21G basis set only upon applying “loose” convergence criteria, and hence, it was not used for further evaluation of the properties). To compare the properties of this octamer with smaller foldamers, additional single-point calculations were carried out at the B3LYP/6-311G(d, p) level (represented as B3LYP/6-311G(d, p)//B3LYP/3-21G). To confirm minima obtained from geometry optimization of crystal structures, several other possible conformers were built and minimized at the same level of theory. Details of the conformations and their corresponding energy differences are provided in the Supporting Information (Schemes S1–S3 and Tables S2–S4). We observed that there were several low-energy isomers, but the lowest energy conformers obtained from these computations were similar to the crystal structures. Overlays of minimum-energy conformers of the oligoamides obtained with the B3LYP/6-311G(d, p) and MO6-2X/6-31G(d, p) basis sets and

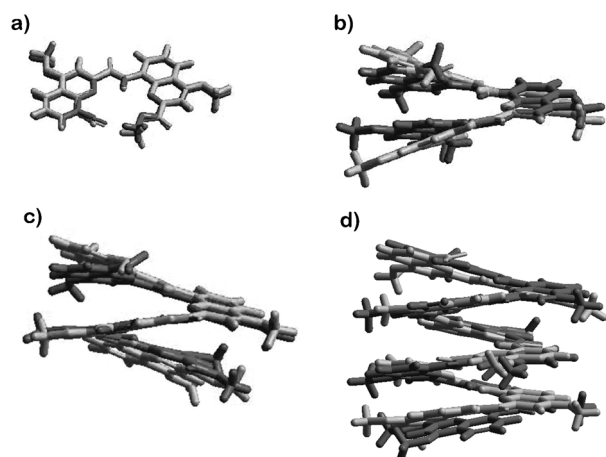


**Figure 3.** Overlaid geometries of a)  $O_2N-Q_2-OMe$ , b)  $O_2N-Q_3-OMe$ , c)  $O_2N-Q_4-OMe$ , and d)  $O_2N-Q_8-OMe$  derived from X-ray crystal structures (dark gray) and energy-minimized structures (light gray) calculated with B3LYP/6-311G(d, p) (a–c) and B3LYP/3-21G basis sets (d). Bromine atoms and isobutoxy side chains from the crystal structures have been replaced (see text).

X-ray structures of the brominated derivatives had a close geometrical resemblance (Figure 3 and Figure S1 in the Supporting Information).<sup>[49,50]</sup> The quinoline dimer,  $O_2N-Q_2-OMe$ , has a crescent shape with a nearly planar structure (Figure 3 a). The helical conformation for the foldamers starts with the trimer,  $O_2N-Q_3-OMe$ . Because we do not have the crystal structure of non-brominated molecules, a direct comparison of the calculated geometrical parameters and the experimental data is not possible. Nevertheless, to understand the effect of substitutions, we have tabulated the most important calculated geometrical parameters in the Supporting Information (Table S5) and also presented pictures of overlays of various substituted tetramers (Figure S2). We conclude from this section that electronic effects associated with bromine substituents or terminal groups have little influence on the geometry of the helix; the minor observed changes might be attributed to steric effects.

## 2.2. Electronic Effects on Bromination

For electrophilic bromination reactions, when electronic effects are dominant, the formation of a bromonium ion intermediate is expected at the C5 position of Q. To verify this, we considered the nitro trimer ( $O_2N-Q_3-OMe$ ) as an example and calculated the stability of potential bromonium ion intermediates with relative internal energies and free energies, including solvent effects. Indeed, it is known that the solvent polarity exerts an important influence on the structure: to explicitly take into account solvent polarity effects, we have adopted a self-consistent reaction field (SCRf) approach with sequential molecular dynamics (SMD),<sup>[51]</sup> as implemented in Gaussian 09. Theoretically, there are four free positions in each quinoline ring (C3, C5, C6, and C7) for bromination (Scheme 1). Quinoline–bromonium ion intermediates with bromine in all possible positions (Figure 4) were modeled and their relative stabilities computed at the B3LYP/6-31G(d, p) and MO6-2X/6-31G(d, p) level of theory; results are presented in Table 1. Approaches from

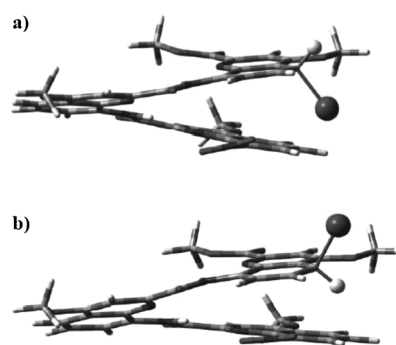


**Figure 4.** Attack by a bromine cation from below (a) or above (b) to form a trimer-bromonium ion intermediate. The dark gray ball indicates the bromine atom.

above and below give rise to diastereomeric intermediate conformers that are unlikely to be identical (Figure 4). The relative energies clearly indicate that the C5 position, as expected, is lower in energy than the other sites both in the gas phase and in solvent. Among the three C5 positions of the quinoline trimer, Q3–C5 is the lowest in energy and is the preferred site of reaction over the Q2–C5 position (the Q1–C5 position is not favorable due to the strong electron-withdrawing nitro group). These calculations indeed show that electronic effects are dominant and the results are in agreement with the experimental observation that Q3–C5 is selectively brominated in this trimer.

## 2.3. Local Nucleophilic Indices

The Fukui function model (LNI) was applied;<sup>[40–47]</sup> this quantifies the local nucleophilicity of the reaction sites. Moreover, it is a well-validated model for various properties, starting from simple organic reactions to enzyme catalysis through to toxicity studies.<sup>[33–47]</sup> The LNI calculated by the conceptual DFT method for the trimer is in agreement with the results of the bromonium ion intermediate, indicating that this model can be applied to such reactions. To probe the regioselectivity in higher oligoamides further, only the conceptual DFT method was applied.

For each oligomer, LNI values were calculated at the B3LYP/6-311G(d, p) level of theory for only the C5 atom of each quinoline ring (Schemes 1 and 2) because it is the site of bromination.<sup>[28]</sup> We found that LNI values (Table 2) were very good descriptors for predicting the most reactive sites of aromatic nuclei towards electrophilic attack. The calculated LNIs for  $O_2N-Q_2-OMe$  (Table 2, entry 1) indicate that the Q2 ring (numbering is given from the N to C terminus) should be more reactive than the Q1 ring (LNI of 0.252 compared with 0.022). The presence of the 8-nitro group on the Q1 ring is the main cause of its low reactivity. The LNI values for  $O_2N-Q_3-OMe$  (Table 2, entry 2) are 0.019, 0.116, and 0.194 at the first, second, and third Q rings, respectively, indicating the more nucleophilic nature of the Q3 ring followed by the Q2 ring. This result predicts the experimentally observed regioselective ESR at Q3, although Q2 is probably less hindered. In the case of  $O_2N-Q_4-$

**Table 1.** Relative stabilities of reaction intermediates (quinoline trimer–bromonium ion) calculated with the B3LYP/6-31G(d, p) basis set. Results with the MO6-2X/6-31G(d, p) basis set are presented in parentheses.

Position	Gas phase				In CH <sub>2</sub> Cl <sub>2</sub> <sup>[a]</sup>	
	(attack from above)		(attack from below)		(attack from above)	(attack from below)
	$\Delta E^{[b]}$	$\Delta G^{[b]}$	$\Delta E^{[b]}$	$\Delta G^{[b]}$	$\Delta E^{[b]}$	$\Delta E^{[b]}$
Q1–C7	39.9 (48.5)	38.5 (48.5)	NA (NA)	NA (NA)	39.9 (47.3)	NA (NA)
Q1–C6	32.2 (37.0)	31.6 (36.6)	30.4 (36.8)	29.8 (37.1)	27.4 (32.5)	27.0 (29.5)
Q1–C5	34.8 (40.8)	35.3 (41.4)	34.8 (44.6)	33.6 (44.9)	34.7 (38.6)	34.4 (42.7)
Q1–C3	22.8 (22.2)	24.1 (24.0)	25.8 (31.9)	24.9 (32.2)	19.1 (18.2)	19.2 (24.1)
Q2–C7	10.9 (14.3)	12.8 (14.5)	10.9 (11.4)	11.2 (12.7)	10.0 (12.4)	7.9 (10.2)
Q2–C6	20.6 (28.5)	19.4 (27.6)	21.1 (28.8)	19.8 (28.8)	17.0 (23.3)	17.5 (23.5)
Q2–C5	7.08 (8.3)	6.6 (9.3)	6.7 (8.1)	6.6 (9.2)	2.6 (5.2)	2.3 (4.9)
Q2–C3	16.2 (20.2)	15.2 (20.4)	15.7 (20.4)	14.9 (19.6)	12.7 (16.2)	12.5 (16.2)
Q3–C7	5.5 (5.2)	5.5 (5.9)	6.2 (8.1)	6.5 (8.6)	6.7 (6.6)	7.3 (8.7)
Q3–C6	NA (NA)	NA (NA)	NA (28.1)	NA (27.17)	NA (NA)	NA (23.5)
Q3–C5	0.2 (1.6)	0 (2.5)	0(0)	0.49 (0)	0.5 (1.9)	0 (0)
Q3–C3	12.9 (18.1)	13.5 (17.6)	14.6 (18.8)	14.5 (18.7)	13.5 (17.2)	12.5 (15.5)

[a] Single-point energy calculations performed for the reaction intermediate in CH<sub>2</sub>Cl<sub>2</sub> (more details are given in the text). NA: results were not obtained due to convergence problems. [b] Relative energy in kcal mol<sup>-1</sup> with respect to Q3–C5.

**Table 2.** Theoretically predicted LNI of various quinoline oligoamides obtained with the B3LYP/6-311G(d, p) basis set. Results for the MO62X/6-31G(d, p) basis set are given in parentheses.<sup>[a]</sup>

Entry	Oligomer <sup>[b]</sup>	Conformer	Q1–C5	Q2–C5	Q3–C5	Q4–C5	Q5–C5	Q6–C5	Q7–C5	Q8–C5
1	O <sub>2</sub> N–Q <sub>2</sub> – OMe	crescent	0.022 (0.076)	<i>0.252</i> ( <i>0.365</i> )	–	–	–	–	–	–
2	O <sub>2</sub> N–Q <sub>3</sub> – OMe	folded	0.019 (0.017)	0.116 (0.038)	<i>0.194</i> ( <i>0.249</i> )	–	–	–	–	–
3	O <sub>2</sub> N–Q <sub>4</sub> – OMe	folded	0.016 (0.029)	0.088 (0.020)	<i>0.393</i> ( <i>0.166</i> )	0.096 (0.058)	–	–	–	–
4	O <sub>2</sub> N–Q <sub>6</sub> – OMe <sup>[c]</sup>	folded	0.012	0.047	<i>0.086</i>	0.056	0.051	0.039	0.054	0.039
5	NC–Q <sub>4</sub> – OMe	folded	0.017 (0.019)	0.098 (0.014)	<i>0.174</i> ( <i>0.296</i> )	0.100 (0.049)	–	–	–	–
6	Ac–Q <sub>4</sub> – OMe	folded	<i>0.105</i> ( <i>0.138</i> )	<i>0.102</i> ( <i>0.024</i> )	<i>0.114</i> ( <i>0.141</i> )	<i>0.091</i> ( <i>0.095</i> )	–	–	–	–
7	NC–Q <sub>2</sub> – OMe	crescent	0.009 (0.032)	<i>0.296</i> ( <i>0.266</i> )	–	–	–	–	–	–
8	Ac–Q <sub>2</sub> – OMe	crescent	<i>0.166</i> ( <i>0.177</i> )	<i>0.17</i> ( <i>0.190</i> )	–	–	–	–	–	–

[a] Numbers in italic indicate the preferred reaction site. [b] Abbreviated names, O<sub>2</sub>N–, NC–, and so forth replace the terminal NH group. [c] Geometry optimization at the B3LYP/3-21G level and LNI calculated at the B3LYP/6-311G(d, p) level.

OMe (Table 2, entry 3), computed LNI values are 0.016, 0.088, 0.393, 0.096 for rings Q1–Q4, respectively. The Q3 ring again possesses a higher LNI than that of the other rings, consistent with experimental evidence, showing that ESR occurs preferentially at that position. Consistent results were also observed for O<sub>2</sub>N–Q<sub>6</sub>–OMe (Table 2, entry 4). Computed LNI values reveal that the Q3 ring is the most nucleophilic (LNI=0.086) when compared with the remaining seven quinoline rings of this oligoamide.

Thus, computed LNI values provide a preliminary insight into how the nucleophilic character is distributed over various sites of the lowest energy conformers (crescent/folded) of quinoline oligoamides of various lengths with the same N- and C-terminal functional groups. It should be noted that LNI

values only provide a qualitative estimate of the relative reactivity at various sites of a given molecule. Variations in the LNI cannot be directly transcribed to a quantitative assessment of relative reaction rates. Furthermore, LNI values of different molecules cannot be subjected to a direct comparison.<sup>[39]</sup> Thus, the results shown in Table 2 do not provide information about the relative ESR rates of the various oligomers.

The experimentally observed effects of varying the substituent at the N terminus were also validated by calculating LNI values (Table 2). When the terminal –NO<sub>2</sub> group is replaced with –CN, as in NC–Q<sub>4</sub>–OMe (Table 2, entry 5), LNI values indicate that the Q3 ring should again be the

most reactive site (LNI=0.174), as observed in the experiments. Both the –CN and –NO<sub>2</sub> groups are electron withdrawing in nature and allow the same regioselectivity despite their structural differences. On the contrary, when –NHAc is introduced instead of –NO<sub>2</sub> (Ac–Q<sub>4</sub>–OMe, Table 2, entry 6), all quinoline rings have similar LNI values: 0.105, 0.102, 0.114, 0.091 from ring Q1 to ring Q4, respectively. LNI values predict poorly selective ESRs on this compound and experiments indeed revealed that a complex mixture of products was generated.<sup>[28]</sup> LNI values were also calculated with the MO6-2X/6-31G(d, p) basis set for validation of the data (Table 2). The results indicate similar trends to those found at the B3LYP/6-311G(d, p) level of theory.

The mechanism through which the effects of the electron-withdrawing groups are responsible for a high regioselectivity is unclear. The N-terminal substituent is remote from the favored reaction site on the Q3 ring through bonds, but it is close in space.<sup>[28]</sup> The fact that LNIs corroborate experimental results suggests that the effect of the terminal substituent operates in the ground state and the unusual regioselectivity may be due to electronic effects modified through folding and not due to steric effects.

## 2.4. MO Analysis

In an attempt to further increase our understanding of the structural principles and substitution effects that determine regioselectivity in helical oligoamides, MOs of the two tetramers with an N-terminal electron-withdrawing group ( $O_2N-Q_4-OMe$ ) and a weak electron-donating group ( $Ac-Q_4-OMe$ ) were generated. To understand the role of folding, only two additional hypothetical conformations were considered, although various conformers exist theoretically. These are the two geometrically distinct conformers, namely, linear and misfolded (Figure 5). Linear conformers were built by rotating all three aryl-carboxamide bonds by  $180^\circ$ , while keeping all amide bonds in a *trans* conformation and all amide protons hydrogen bonded to the nitrogen atoms of the quinoline ring to which they belong. It has to be kept in mind that this only represents a completely unwound helix and it does not have to be the lowest energy linear conformation. Misfolded conformers were constructed by simply rotating the aryl-carboxamide bond of Q1 ring by  $180^\circ$ . The geometries of all of these conformers were optimized at the B3LYP/6-311G(d, p) level of theory. Based on the electronic energy differences, it was found, in general, that the folded conformer was the most stable one, followed by the misfolded conformer, and then the linear conformer (Table 3). The optimized geometries of the linear and misfolded conformers are given in the Supporting Information.

MOs of the molecules (HOMO-1 to LUMO) were gen-

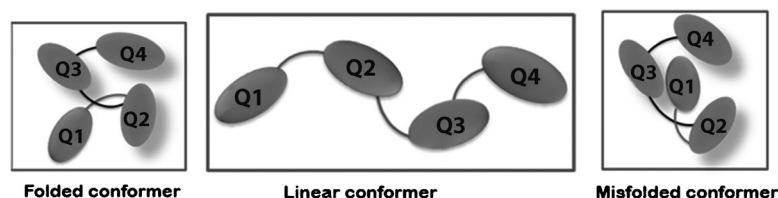


Figure 5. Selected conformers of the oligoamides.

Table 3. Relative electronic energies,  $\Delta E$  (with respect to the lowest energy conformation), and dipole moments,  $\mu$ , of selected conformers of various oligoamides obtained with the B3LYP/6-311G(d, p) basis set. Results for the MO62X/6-31G(d, p) basis set are given in parentheses.

Oligoamide	Folded		Misfolded		Linear	
	$\Delta E^{[a]}$	$\mu^{[b]}$	$\Delta E^{[a]}$	$\mu^{[b]}$	$\Delta E^{[a]}$	$\mu^{[b]}$
$O_2N-Q_4-OMe$	0.0 (0.0)	5.9 (4.7)	7.9 (6.8)	7.8 (8.0)	17.0 (40.5)	21.9 (22.5)
$Ac-Q_4-OMe$	0.0 (0.0)	7.4 (6.2)	5.2 (6.6)	7.0 (9.2)	20.0 (41.3)	20.8 (20.9)
$H_2N-Q_4-OMe$	0.0 (0.0)	4.4 (4.1)	6.6 (7.8)	2.6 (2.3)	15.0 (40.0)	16.4 (16.8)
$O_2N-Q_8-OMe^{[c]}$	0.0	6.4	–	–	23.8	59.9
$Ac-Q_8-OMe^{[c]}$	0.0	5.99	–	–	20.6	58.1

[a] In kcal mol<sup>-1</sup>. [b] In Debye. [c] Obtained at the B3LYP/6-311G(d,p)//B3LYP/3-21G level.

erated at the B3LYP/6-311G(d, p) level of theory and are shown in Figures 6 to 9, while the other MOs are shown in the Supporting Information (Figures S3–S12). MO analysis shows that, in the hypothetical linear conformation of  $O_2N-Q_4-OMe$ , the HOMO is localized on the Q2 ring; HOMO-1 is on the Q3 ring (Figure 6). On the other hand, the LUMO is localized on the Q4 ring with slight delocalization and the LUMO + 1 is largely delocalized on the entire molecule. Upon folding, the electron density in the HOMO accumulates on the Q3 ring. Moreover, the HOMO of the folded conformer of  $O_2N-Q_4-OMe$  ( $-5.47$  eV) is more destabilized compared with the linear conformer ( $-5.80$  eV). The LUMO on the other hand is now largely localized on the first ring, while again in this case the LUMO +

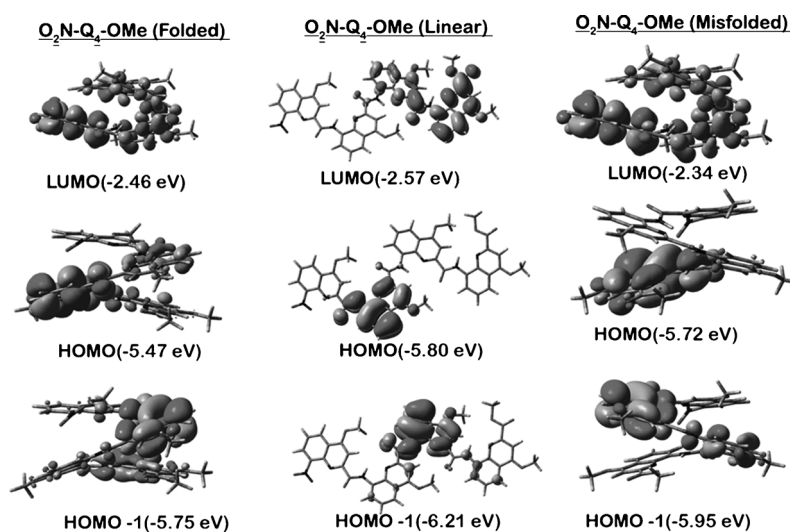


Figure 6. FMOs of selected conformers of  $O_2N-Q_4-OMe$  obtained at the B3LYP/6-311G(d,p) level. For convenience, the  $O_2N$ - group replaces the terminal NH group.

1 is also delocalized. The LUMO is also destabilized from  $-2.57$  eV in the linear molecule to  $-2.46$  eV in the folded one. To confirm whether destabilization was due to folding, the FMO of the hypothetical misfolded conformer was considered. It was found that the HOMO ( $-5.72$  eV) was slightly destabilized relative to the linear conformer, but stabilized with respect to the folded conformer. In the misfolded conformation, the HOMO is localized on the Q4 ring (Figure 6). Here, the LUMO is also destabilized, but not as much as that in the folded molecule. LUMO and the LUMO + 1 are delocalized over the entire molecule, unlike the occupied orbitals. Destabilization of the orbitals presumably occurs due to the through-space interactions between the  $\text{NO}_2$  group and the orbitals of the backbone upon folding.

On the contrary, in the case of folded  $\text{Ac-Q}_4\text{-OMe}$ , the HOMO ( $-5.66$  eV) is slightly stabilized compared with the linear conformer ( $-5.54$  eV) (Figure 7), while the HOMO of the misfolded conformation has even greater stabilization ( $-5.70$  eV). Spreading of the electron density over the entire backbone of  $\text{Ac-Q}_4\text{-OMe}$  is observed in the HOMO and HOMO-1 of the folded conformer, as opposed to the linear conformer of  $\text{Ac-Q}_4\text{-OMe}$ . Additionally, near degeneracy (0.05 eV difference in energy) of HOMO and HOMO-1 in the folded conformer is observed. The LUMO and LUMO + 1 in the folded and misfolded case are delocalized, unlike the linear one. This demonstrates a stronger effect of substituents on the folded conformers over the other (unfolded) conformers.

To further investigate this observation, an oligoamide of the same series containing a strong electron-donating group,  $\text{H}_2\text{N-Q}_4\text{-OMe}$  (Figures S9–S12 in the Supporting Information), was considered for similar calculations. As with  $\text{Ac-Q}_4\text{-OMe}$ , we observed increasing stability of the orbitals upon folding. For example, in the linear conformation, the HOMO lies at  $-5.01$  eV, while for the folded and misfolded conformations the HOMO energies are  $-5.19$  and  $-5.23$  eV, respectively. The donating group reinforces the stabilization of the HOMO in the folded conformer, which is then localized on the Q1 ring in all the three cases. This clearly indicates that this would be the site of electrophilic substitution.

We also analyzed the orbitals of the octamer, but only for the folded and linear conformers of  $\text{O}_2\text{N-Q}_8\text{-OMe}$  (Figure 8) and  $\text{Ac-Q}_8\text{-OMe}$  (Figure 9) obtained at the B3LYP/6-311G(d, p)//B3LYP/3-21G level. The behavior was similar to that of the tetramers and the orbitals were of a similar nature. Significant delocalization is observed in the case of the folded conformation with the weak donor (terminal  $\text{AcNH-}$ ). Like in the tetramer case, the HOMO-1 is almost degenerate and the orbitals

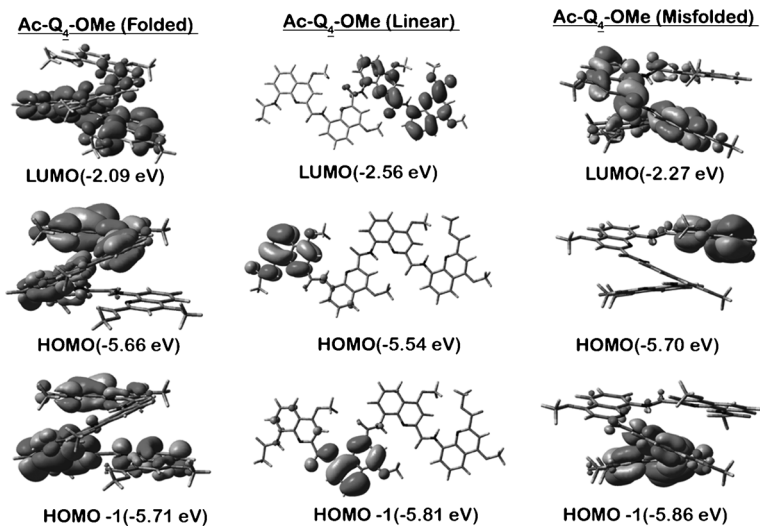


Figure 7. FMOs of selected conformers of  $\text{Ac-Q}_4\text{-OMe}$  obtained at the B3LYP/6-311G(d,p) level.

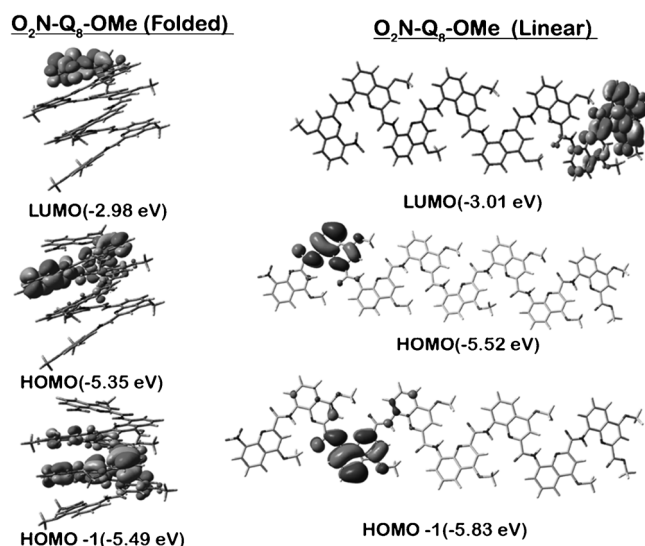
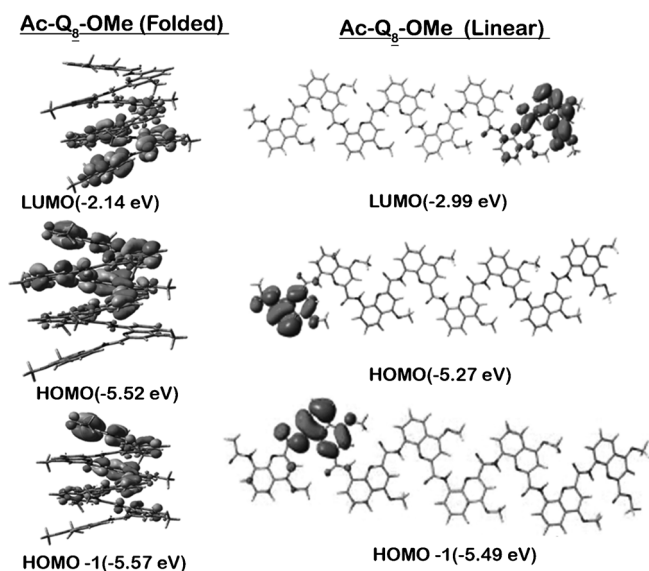


Figure 8. FMOs of selected conformers of  $\text{O}_2\text{N-Q}_8\text{-OMe}$  obtained at the B3LYP/6-311 G(d, p)//B3LYP/3-21G level.

are stabilized. For  $-\text{NO}_2$ , the orbitals are destabilized upon folding and the delocalization is of a similar nature to that of the tetramer case. The LUMO is largely delocalized on the weak donor (terminal  $\text{AcNH-}$ ). Moreover, there is a very good correlation with smaller oligoamides, such as tetramers, and it is presumed that the same trends would be reproduced even with longer oligoamides.

In general, we observe that, in all linear conformers (where mesomeric and inductive effects can play a direct role), there is a slight delocalization of electron density in the LUMO, but not in the HOMO. Upon folding, we notice delocalization in the HOMO and HOMO-1 in the case of fully folded conformers. This can be attributed to folding, which mixes up the orbitals of the linear conformer due to stronger coupling of the orbitals of the backbone with each other. Even greater delocali-



**Figure 9.** FMOs of selected conformers of Ac-Q<sub>8</sub>-OMe obtained at the B3LYP/6-311G(d,p)//B3LYP/3-21G level.

zation is noted in the LUMOs upon folding for H<sub>2</sub>N-Q<sub>4</sub>-OMe and Ac-Q<sub>4</sub>-OMe compared with O<sub>2</sub>N-Q<sub>4</sub>-OMe. Large LNI values are obtained for those monomers in which the HOMO is localized. Slightly smaller LNI values are obtained when the HOMO-1 is localized. The larger contribution from the Q2, Q3, and Q4 rings in Ac-Q<sub>4</sub>-OMe is due to the small energy gap between the HOMO and HOMO-1. To predict the reactive sites in the linear conformers, LNI values were calculated and are presented in Table 4. The largest LNI is found on the Q2

<b>Table 4.</b> Theoretically predicted LNIs of two quinoline oligoamides (linear conformations).				
Oligoamide <sup>[a]</sup>	LNI <sup>[b]</sup>			
	Q <sub>1</sub> -C <sub>5</sub>	Q <sub>2</sub> -C <sub>5</sub>	Q <sub>3</sub> -C <sub>5</sub>	Q <sub>4</sub> -C <sub>5</sub>
O <sub>2</sub> N-Q <sub>4</sub> -OMe	0.007	<i>0.164</i>	0.080	0.082
(linear)	(0.001)	( <i>0.286</i> )	(0.040)	(0.017)
Ac-Q <sub>4</sub> -OMe	<i>0.139</i>	0.102	0.057	0.057
(linear)	( <i>0.256</i> )	(0.073)	(0.021)	(0.011)

[a] Geometry optimization and LNI calculations at the B3LYP/6-311G(d, p) level. Results for the MO62X/6-31G(d, p) basis set are given in parentheses. [b] Numbers in italic indicate the preferred reaction site.

ring of linear O<sub>2</sub>N-Q<sub>4</sub>-OMe (-0.164 eV), which is where the HOMO (-5.8 eV) is localized. In case of the linear Ac-Q<sub>4</sub>-OMe, a larger LNI is found on the Q1 ring (0.139), which is where the HOMO is localized, followed by on the Q2 ring (0.102) where the HOMO-1 is localized. Moreover, the difference in LNI between the highest (Q1 ring) and second highest (Q2 ring) is 0.037, which is smaller than that for O<sub>2</sub>N-Q<sub>4</sub>-OMe (a difference of 0.082 between Q1, Q3, and Q4). The energy difference between the HOMO (5.54 eV) and HOMO-1 (5.81 eV) of linear Ac-Q<sub>4</sub>-OMe is about 0.27 eV and this large gap reduces the effect of HOMO-1 relative to that of the folded conformer. In

summary, folding changes the orbital energy levels and coupling of the substituents with orbitals of the backbone. The latter effect is presumably due to through-space interactions, but, interestingly, it is dependent on the nature of the N-terminal substituent. In the case of electron-withdrawing groups, the orbitals destabilize upon folding, whereas the opposite is true with electron-donating groups.

### 3. Conclusions

Our computational study demonstrated important electronic effects associated with the folding of an oligomer through noncovalent interactions. Quinoline oligoamides are prone to fold into helical conformations and the energy difference between the helical and linear conformers is high. Thus, it seems that there is less scope for the existence of other conformers. Calculations confirmed the experimentally observed regioselectivity of these helical oligomers towards aromatic electrophilic substitutions and also the important influence of substituents at the N terminus on this regioselectivity. We have applied, for the first time, the conceptual DFT (LNI) method to study helical oligoamide foldamers. The calculated results exhibited great consistency with experimental results and showed the usefulness of the LNI model for folded architectures. MO analysis revealed the role of both HOMO and HOMO-1. In the case of the NO<sub>2</sub>-terminated foldamer (O<sub>2</sub>N-Q<sub>4</sub>-OMe), the energy gap between HOMO-1 and HOMO was 0.3 eV. Hence, the LNI value of the Q2 and Q4 rings of the folded tetramer in which HOMO-1 is localized is small. On the other hand, in Ac-Q<sub>4</sub>-OMe, the HOMO and HOMO-1 have an energy difference of only 0.05 eV. The HOMO-1 orbitals are localized on the Q1, Q3, and Q4 rings and the HOMO is localized on the Q1, Q2, and Q3 rings. Hence, the LNI values of all of the monomers are quite large. The present theoretical investigation gave promising insight into understanding folding-induced reactivity and laid the foundations for engineering reactivity in synthetic folded architectures, eventually paving the way to the long-term goal of designing artificial enzymes. Furthermore, it highlights the relevance of a hand-in-hand approach for computational and experimental investigations to promote foldamer research.<sup>[49,50,52-57]</sup> Although the present study dealt with unusual regioselectivity in foldamers, future work will be dedicated to investigating the reaction rates when the length of the oligoamide increases and also the effect of remote substituents on the backbone.

### Acknowledgements

We thank Project Director, NIPER-Hyderabad and Director, IICT, for constant support.

**Keywords:** computational chemistry · density functional theory · foldamers · quinoline oligoamides · regioselectivity

[1] P. E. Nielsen, M. Egholm, R. H. Berg, O. Buchardt, *Science* **1991**, *254*, 1497.

- [2] R. J. Simon, R. S. Kania, R. N. Zuckermann, V. D. Huebner, D. A. Jewell, S. Banville, S. Ng, L. Wang, S. Rosenberg, C. K. Marlowe, D. C. Spellmeyer, R. Tan, A. D. Frankel, D. V. Santi, F. E. Cohen, P. A. Bartlett, *Proc. Natl. Acad. Sci. USA* **1992**, *89*, 9367.
- [3] D. H. Appella, L. A. Christianson, I. L. Karle, D. R. Powell, S. H. Gellman, *J. Am. Chem. Soc.* **1996**, *118*, 13071.
- [4] D. Seebach, M. Overhand, F. N. M. Kuhnle, B. Martinoni, L. Oberer, U. Hommel, H. Widmer, *Helv. Chim. Acta* **1996**, *79*, 913.
- [5] J. C. Nelson, J. G. Saven, J. S. Moore, P. G. Wolynes, *Science* **1997**, *277*, 1793.
- [6] R. S. Lokey, B. L. Iverson, *Nature* **1995**, *375*, 303.
- [7] S. H. Gellman, *Acc. Chem. Res.* **1998**, *31*, 173.
- [8] *Foldamers: Structure, Properties and Applications* (Eds.: S. Hecht, I. Huc). Wiley-VCH, Weinheim, **2007**.
- [9] D. J. Hill, M. J. Mio, R. B. Prince, T. S. Hughes, J. S. Moore, *Chem. Rev.* **2001**, *101*, 3893.
- [10] I. Huc, *Eur. J. Org. Chem.* **2004**, 17.
- [11] I. Saraogi, A. D. Hamilton, *Chem. Soc. Rev.* **2009**, *38*, 1726.
- [12] G. Guichard, I. Huc, *Chem. Commun.* **2011**, *47*, 5933, and references cited therein.
- [13] Q. Gan, Y. Ferrand, B. Kauffmann, C. Bao, A. Grelard, H. Jiang, I. Huc, *Science* **2011**, *331*, 1172.
- [14] S. Choi, A. Isaacs, D. Clements, D. Liu, H. Kim, R. W. Scott, J. D. Winkler, W. F. DeGrado, *Proc. Natl. Acad. Sci. USA* **2009**, *106*, 6968.
- [15] C. Dolain, H. Jiang, J. M. Leger, P. Guionneau, I. Huc, *J. Am. Chem. Soc.* **2005**, *127*, 12943.
- [16] P. Lafite, F. Andre, D. C. Zeldin, P. M. Dansette, M. Mansuy, *Biochemistry* **2007**, *46*, 10237.
- [17] O. Kundrat, H. Dvorakova, V. Eigner, P. Lhotak, *J. Org. Chem.* **2010**, *75*, 407.
- [18] T. Hosoya, Y. Nakao, H. Sato, S. Sakaki, *J. Org. Chem.* **2010**, *75*, 8400.
- [19] A. Cavarzan, A. Scarso, P. Sgarbossa, G. Strukul, J. N. H. Reek, *J. Am. Chem. Soc.* **2011**, *133*, 2848.
- [20] W. Fudickar, T. Linker, *Chem. Commun.* **2008**, 1771.
- [21] S. Rieth, K. Hermann, B. Y. Wang, J. D. Badjic, *Chem. Soc. Rev.* **2011**, *40*, 1609.
- [22] R. A. Smaldone, J. S. Moore, *J. Am. Chem. Soc.* **2007**, *129*, 5444.
- [23] H. P. Yi, J. Wu, K. L. Ding, X. K. Jiang, Z. T. Li, *J. Org. Chem.* **2007**, *72*, 870.
- [24] P. S. Baran, T. J. Maimone, J. M. Richter, *Nature* **2007**, *446*, 404.
- [25] D. A. Guthrie, J. D. Tovar, *Org. Lett.* **2008**, *10*, 4323.
- [26] D. A. Guthrie, J. D. Tovar, *Chem. Eur. J.* **2009**, *15*, 5176.
- [27] W. Zhong, J. P. Gallivan, Y. Zhang, L. Li, H. A. Lester, D. A. Dougherty, *Proc. Natl. Acad. Sci. USA* **1998**, *95*, 12088.
- [28] K. Srinivas, B. Kauffmann, C. Dolain, J. M. Leger, L. Ghosez, I. Huc, *J. Am. Chem. Soc.* **2008**, *130*, 13210.
- [29] J. M. Heemstra, J. S. Moore, *J. Am. Chem. Soc.* **2004**, *126*, 1648.
- [30] C. Dolain, C. Zhan, J.-M. Leger, L. Daniels, I. Huc, *J. Am. Chem. Soc.* **2005**, *127*, 2400.
- [31] H.-Y. Hu, J. F. Xiang, J. Cao, C.-F. Chen, *Org. Lett.* **2008**, *10*, 5035.
- [32] B. Qin, L. Jiang, S. Shen, C. Sun, W. Yuan, S. F. Y. Li, H. Zeng, *Org. Lett.* **2011**, *13*, 6212.
- [33] R. Lonsdale, K. E. Ranaghan, A. J. Mulholland, *Chem. Commun.* **2010**, *46*, 2354.
- [34] A. Warshel, P. K. Sharma, M. Kato, Y. Xiang, H. Liu, M. H. M. Olsson, *Chem. Rev.* **2006**, *106*, 3210.
- [35] G. Roos, P. Geerlings, J. Messens, *J. Phys. Chem. B* **2009**, *113*, 13465.
- [36] R. G. Parr, W. Yang, *Annu. Rev. Phys. Chem.* **1995**, *46*, 701.
- [37] P. Geerlings, F. De Proft, W. Langenaeker, *Chem. Rev.* **2003**, *103*, 1793.
- [38] R. K. Roy, S. Saha, *Annu. Rep. Prog. Chem. Sect. C* **2010**, *106*, 118.
- [39] H. Chermette, *J. Comput. Chem.* **1999**, *20*, 129.
- [40] D. R. Roy, U. Sarkar, P. K. Chattaraj, A. Mitra, J. Padmanabhan, R. Parthasarathi, V. Subramanian, V. Damme, P. Bultinck, *Mol. Diversity* **2006**, *10*, 119.
- [41] S. Catak, M. D'hooghe, T. Verstraelen, K. Hemelsoet, A. V. Nieuwenhove, H.-J. Ha, M. Waroquier, N. De Kimpe, V. Speybroeck, *J. Org. Chem.* **2010**, *75*, 4530.
- [42] S. Pratihari, S. Roy, *J. Org. Chem.* **2010**, *75*, 4957.
- [43] J. Khandogin, K. Musier-Forsyth, D. M. York, *J. Mol. Biol.* **2003**, *330*, 993.
- [44] L. R. Domingo, E. Chamorro, P. Pérez, *Eur. J. Org. Chem.* **2009**, 3036.
- [45] L. R. Domingo, T. Picher, J. A. Saez, *J. Org. Chem.* **2009**, *74*, 2726.
- [46] J. A. H. Schwöbel, Y. K. Koleva, S. J. Enoch, F. Bajot, M. Hewitt, J. C. Madden, D. W. Roberts, T. W. Schultz, M. T. D. Cronin, *Chem. Rev.* **2011**, *111*, 2562.
- [47] R. G. Parr, W. T. Yang, *J. Am. Chem. Soc.* **1984**, *106*, 4049.
- [48] Gaussian 09, Revision B.01, M. J. Frisch, G. W. Trucks, H. B. Schlegel, G. E. Scuseria, M. A. Robb, J. R. Cheeseman, G. Scalmani, V. Barone, B. Menonucci, G. A. Petersson, H. Nakatsuji, M. Caricato, X. Li, H. P. Hratchian, A. F. Izmaylov, J. Bloino, G. Zheng, J. L. Sonnenberg, M. Hada, M. Ehara, K. Toyota, R. Fukuda, J. Hasegawa, M. Ishida, T. Nakajima, Y. Honda, O. Kitao, H. Nakai, T. Vreven, J. A. Montgomery, Jr., J. E. Peralta, F. Ogliaro, M. Bearpark, J. J. Heyd, E. Brothers, K. N. Kudin, V. N. Staroverov, R. Kobayashi, J. Normand, K. Raghavachari, A. Rendell, J. C. Burant, S. S. Iyengar, J. Tomasi, M. Cossi, N. Rega, N. J. Millam, M. Klene, J. E. Knox, J. B. Cross, V. Bakken, C. Adamo, J. Jaramillo, R. Gomperts, R. E. Stratmann, O. Yazyev, A. J. Austin, R. Cammi, C. Pomelli, J. W. Ochterski, R. L. Martin, K. Morokuma, V. G. Zakrzewski, G. A. Voth, P. Salvador, J. J. Dannenberg, S. Dapprich, A. D. Daniels, O. Farkas, J. B. Foresman, J. V. Ortiz, J. Cio-slowski, D. J. Fox, Gaussian, Inc., Wallingford, CT, **2010**.
- [49] L. Ducasse, F. Castet, A. Fritsch, I. Huc, T. Buffeteau, *J. Phys. Chem. A* **2007**, *111*, 5092.
- [50] T. Buffeteau, L. Ducasse, L. Poniman, N. Delsuc, I. Huc, *Chem. Commun.* **2006**, 2714.
- [51] A. V. Marenich, C. J. Cramer, D. G. Truhlar, *J. Phys. Chem. B* **2009**, *113*, 6378.
- [52] B. Zhang, T. Yuan, H. Jiang, M. Lei, *J. Phys. Chem. B* **2009**, *113*, 10934.
- [53] I. V. Korendovych, Y. H. Kim, A. H. Ryan, J. D. Lear, W. F. DeGrado, S. J. Shandler, *Org. Lett.* **2010**, *12*, 5142.
- [54] H. Dong, S. Hua, S. Li, *J. Phys. Chem. A* **2009**, *113*, 1335.
- [55] S. P. Elmer, V. S. Pande, *J. Chem. Phys.* **2004**, *121*, 12760.
- [56] S. J. Shandler, M. V. Shapovalov, R. L. Dunbrack, Jr., W. F. DeGrado, *J. Am. Chem. Soc.* **2010**, *132*, 7312.
- [57] Z. Lin, A. Teslja, V. Pophristic, *J. Comput. Chem.* **2011**, *32*, 1846.

Received: May 16, 2012

Published online on August 7, 2012